Acceleration statistics of finite-sized particles in turbulent flow: the role of Faxén forces

By E. CALZAVARINI[1], R. VOLK[1], M. BOURGOIN[2], E. LÉVÊQUE[1], J.-F. PINTON[1], F. TOSCHI[3]

[1]Laboratoire de Physique de École Normale Supérieure de Lyon, CNRS et Université de Lyon, 46 Allée d'Italie, 69007 Lyon, France.
[2]Laboratire des Écoulements Géophysiques et Industriels, CNRS/UJF/INPG UMR5519, BP53, 38041 Grenoble, France.
[3]Dept. Physics and Dept. Mathematics & Computer Science, Eindhoven University of Technology, P.O. Box 513, 5600 MB Eindhoven, Netherlands

(International Collaboration for Turbulence Research)

(Received 26 November 2008)

The dynamics of particles in turbulence when the particle-size is larger than the dissipative scale of the carrier flow is studied. Recent experiments have highlighted signatures of particles finiteness on their statistical properties, namely a decrease of their acceleration variance, an increase of correlation times -at increasing the particles size- and an independence of the probability density function of the acceleration once normalized to their variance. These effects are not captured by point particle models. By means of a detailed comparison between numerical simulations and experimental data, we show that a more accurate model is obtained once Faxén corrections are included.

The study of Lagrangian turbulence and of turbulent transport of material particles has received growing interest in recent years (Toschi & Bodenschatz (2009)). Modern experimental techniques (based on synchronization of multiple fast cameras, or ultrasonic/laser Doppler velocimetry) allow nowadays to fully resolve particle tracks in turbulent flows (La Porta *et al.* (2001); Mordant *et al.* (2001); Xu *et al.* (2006); Berg (2006); Volk *et al.* (2008*b*)). These techniques have opened the way toward a systematic study of the dynamics of material (or inertial) particles. When the particle density is different from the one of the carrier fluid, a rich phenomenology emerges, such as particle clustering and segregation (Squires & Eaton (1991); Calzavarini *et al.* (2008*b*,*a*)). Numerical studies have proven to be essential tools in complementing and benchmarking early days experimental data: investigations of fluid tracers dynamics have shown remarkable agreement with experiments (Mordant *et al.* (2004); Arneodo *et al.* (2008); Biferale *et al.* (2008)). Lagrangian numerical studies through Direct Numerical Simulations (DNS) of very small - computationally assumed to be pointwise - particles have also shown encouraging consistency with experimental measurements for inertial particles (Bec *et al.* (2006); Ayyalasomayajula *et al.* (2006); Salazar *et al.* (2008); Volk *et al.* (2008*a*)). However, in many situations the size of the particles is not small with respect to turbulence scales, in particular the dissipative scale η. One example is Plankton which, while neutrally buoyant, cannot be considered as a tracer because of its size in the order of few dissipative scales. Typical marine and atmospherical environmental flows have $\eta \sim O(10)\mu m$.

The statistics of particle accelerations, which directly reflects the action of hydrodynamical forces, has been used to experimentally assess the statistical signature of "large"

spherical particles, i.e. whose diameter D is larger than the smallest turbulence scale η. Recent studies (Voth *et al.* (2002); Qureshi *et al.* (2007)) and detailed comparison between experiments and numerical simulations (Volk *et al.* (2008*a*)) have shown that finite-sized neutrally-buoyant particles cannot be modeled as pointwise in numerical studies. Features which have been clearly associated with a finite particle size are:

i) For neutrally buoyant particles with $D > \eta$ the acceleration variance decreases at increasing the particle size. A scaling law behavior, $\langle a^2 \rangle \sim \varepsilon^{4/3} D^{-2/3}$ (with ε being the energy dissipation rate), has been suggested on the basis of Kolmogorov 1941 (K41) turbulence phenomenology (Voth *et al.* (2002); Qureshi *et al.* (2007)).

ii) The normalized acceleration probability density function (PDF) depends at best very weakly on the particle diameter. Its shape can be fitted with stretched exponential functions (see Voth *et al.* (2002); Qureshi *et al.* (2007)).

iii) The autocorrelation function of acceleration shows increased correlation time with increasing particle-size (Volk *et al.* (2008*a*)).

While experimentally it is easier to study large ($D > \eta$) particles, theoretically (and therefore computationally) this turns out a far more difficult task. Our aim in this article is to study the novel features associated with finite particles size in developed turbulent flows, while presenting an improved numerical model capable to solve most of the discrepancies between experiments and simulations noticed in (Volk *et al.* (2008*a*)). We show that qualitatively and quantitatively the new features are well captured by an equation of motion which takes into account the effect of the nonuniformity of the flow at the particle-scale. To our knowledge the impact on acceleration statistics of such forces, known since a long time as Faxén corrections (Faxén (1922)) has never been considered.

The article is organized as follows. First we comment on the problems of obtaining an equation of motion for finite-sized particles. We examine the approximation on which point-particles equations rely and discuss two highly simplified models for the dynamics of small ($D < \eta$) and finite-sized ($D > \eta$) particles. Section 2 gives the numerical implementation of the proposed Faxén-corrected model. In section 3 we show basic physical differences between the statistics of particle acceleration given by numerics with or without Faxén corrections. Section 4 contains the comparison of the model against experimental results, focusing on neutrally buoyant particles. Finally in Sec. 5 we summarize the results, we critically review the model and discuss how it can be improved.

1. Equation of motion for finite-sized particle in turbulence

Many studies on fine particulate flows have based particle's description on an equation - referred to as Maxey-Riley-Gatignol - which is an exact derivation of the forces on a particle in a nonuniform unsteady flow in the limit of vanishing Reynolds numbers $Re_p = Dv_s/\nu$ and $Re_S = D^2\Gamma/\nu$, where v_s is the slip particle velocity respect to the fluid and $\Gamma = |\nabla \mathbf{u}|$ the typical shear-scale in the flow (Maxey & Riley (1983); Gatignol (1983)). In the net hydrodynamical force acting on a particle given by this equation one recognizes several contributions: the steady Stokes drag, the fluid acceleration force (sum of the pressure gradient and the dissipative forces on the fluid), the added mass, the buoyancy, the history Basset-Boussinesq force, and Faxén corrections. When the control parameters Re_p and Re_S become finite, the non-linearity of the flow dynamics in the vicinity of the particle must be taken into account (see the review by Michaelides (1997)). An expression for the added mass term which is correct at any Re_p value has been derived by Auton *et al.* (1988). But much more complicated is the situation for the other forces involved. The drag term becomes Re_p dependent and empirical expressions based on numerical computations have been proposed (see Clift *et al.* (1978)). Furthermore, a lift

force appears at finite values of Re_p and Re_S. This force is notably hard to model because of the non-linear combination of shear and vorticity, and approximate expressions based on Saffman (small Re_p) and Lighthill-Auton (large Re_p) mechanisms are often used in studies (see e.g. discussion on lift on bubbles by Magnaudet & Legendre (1998)).

Theoretical and numerical studies of fine disperse multi-phase flows, which aim at describing the behavior of a large number of particles, have adopted simplified models where the sub-dominant terms in Maxey-Riley-Gatignol equation are neglected (Balkovsky *et al.* (2001); Bec (2005)). A minimal model, used to address particle Lagrangian dynamics in highly turbulent suspensions, takes into account only a few ingredients: the Stokes drag, the Auton added mass and the fluid acceleration term (Babiano *et al.* (2000); Calzavarini *et al.* (2008*b*)). This leads to:

$$\frac{d\boldsymbol{v}}{dt} = \frac{3\ \rho_f}{\rho_f + 2\ \rho_p}\ \left(\frac{D\mathbf{u}}{Dt} + \frac{3\nu}{a^2}\left(\mathbf{u} - \boldsymbol{v}\right)\right), \tag{1.1}$$

where ρ_f and ρ_p are respectively the fluid and the particle density, ν the fluid kinematic viscosity and a the radius of the particle, which is considered spherical. However, the size of the particle in the above equation is essentially *virtual*. Equation (1.1) contains only a time-scale, namely the particle relaxation time τ_p, which embodies a particle length-scale merely in combination with the kinematic viscosity of the flow and with the densities coefficients, i.e., $\tau_p \equiv a^2(\rho_f + 2\ \rho_p)/(9\nu\rho_f)$. In practice, the drag term in equation (1.1) performs a purely temporal filtering of the flow velocity fluctuations.

It is the role of Faxén terms to account for the non-uniformity of the flow at the particle-size. Faxén forces represent necessary physical corrections when analyzing the behavior of $D > \eta$ particles in turbulence. The Faxén theorem for the drag force on a moving sphere states the relation

$$\mathbf{f}_D = 6\pi\nu\rho_f a\ \left(\frac{1}{4\pi a^2}\int_{S_a} \mathbf{u}(\mathbf{x})\ d\mathbf{S} - \boldsymbol{v}\right) = 6\pi\nu\rho_f a\left(\langle\mathbf{u}\rangle_{S_a} - \boldsymbol{v}\right), \tag{1.2}$$

where the integral is over surface of the sphere and $\mathbf{u}(\mathbf{x})$ the nonhomogeneous steady motion of the fluid in the absence of the sphere. As later shown by Gatignol (1983), Faxén force corrections via sphere volume averages should also be included on the inertial hydrodynamic forces acting on the sphere. In particular the expression for the fluid acceleration and added mass force becomes:

$$\mathbf{f}_A = \frac{4}{3}\pi a^3\rho_f\left(\langle\frac{D\mathbf{u}}{Dt}\rangle_{V_a} + \frac{1}{2}\left(\langle\frac{d\mathbf{u}}{dt}\rangle_{V_a} - \frac{d\boldsymbol{v}}{dt}\right)\right) \tag{1.3}$$

where similarly as above $\langle\ldots\rangle_{V_a}$ denotes the volume average over the spherical particle. Putting together the two force contributions of Eqs. (1.2)-(1.3) into an equation of motion for a sphere, $(4/3)\pi a^3\rho_p\ d\boldsymbol{v}/dt = \mathbf{f}_D + \mathbf{f}_A$, and keeping into account the Auton added mass correction for finite Re_P, i.e., $d\mathbf{u}/dt \to D\mathbf{u}/Dt$, we obtain the phenomenological Faxén-corrected equation of motion:

$$\frac{d\boldsymbol{v}}{dt} = \frac{3\ \rho_f}{\rho_f + 2\ \rho_p}\ \left(\langle\frac{D\mathbf{u}}{dt}\rangle_{V_a} + \frac{3\nu}{a^2}\left(\langle\mathbf{u}\rangle_{S_a} - \boldsymbol{v}\right)\right). \tag{1.4}$$

In the small particle limit, when $\mathbf{u} \simeq \boldsymbol{v}$, corrections can be approximated by Taylor expansion $\langle\mathbf{u}(\mathbf{x},t)\rangle_{S_a} \simeq \mathbf{u} + \frac{a^2}{6}\nabla^2\mathbf{u} + O(a^4)$; $\langle\frac{D\mathbf{u}(\mathbf{x},t)}{Dt}\rangle_{V_a} \simeq \frac{d}{dt}\left(\mathbf{u} + \frac{a^2}{10}\nabla^2\mathbf{u} + O(a^4)\right)$, therefore the first order Faxén correction accounts for the curvature of the unperturbed flow at the particle location. In a turbulent flow the correction term becomes important when $a > \eta$, with a weak Taylor-based Reynolds number Re_λ dependence. With the as-

sumption $\nabla^2 \mathbf{u} \sim 15\mathbf{u}_{rms}/\lambda^2$, where λ is the Taylor microscale, one can roughly estimate $a^2\nabla^2\mathbf{u} \sim 15\mathbf{u}_{rms}\ (a/\lambda)^2 \sim \mathbf{u}_{rms}\ (a/\eta)^2\sqrt{15}/Re_\lambda$.

2. Numerical implementation of particle model and tubulence DNS

We adopt here a further approximation which allows efficient numerical computations of Eq. (1.4). Volume averages at particles' positions are substituted by local interpolations after filtering by a Gaussian envelope with standard deviation, σ, proportional to the particle radius. Gaussian convolutions are then efficiently computed in spectral space, and the Gaussian volume averaged field reads:

$$\langle u_i \rangle_{G,V_\sigma}(\mathbf{x}) = \mathcal{DFT}^{-1}_{(N^3)}\left[\tilde{G}_\sigma(\mathbf{k})\ \tilde{u_i}(\mathbf{k})\right], \tag{2.1}$$

where $\mathcal{DFT}^{-1}_{(N^3)}$ denotes a discrete inverse Fourier transform on a grid N^3, $\tilde{G}_\sigma(\mathbf{k}) = \exp(-\sigma^2\mathbf{k}^2/2)$ is the Fourier transform of a unit volume Gaussian function of variance σ and $\tilde{u_i}(\mathbf{k})$ is the Fourier transform of a vector field (the material derivative of fluid velocity in Eq. (1.4)). The surface average is obtained using the exact relation:

$$\langle u \rangle_{S_a} = \frac{1}{3a^2}\frac{d}{da}\left(a^3\langle \mathbf{u}\rangle_{V_a}\right), \tag{2.2}$$

which leads to:

$$\langle u_i \rangle_{G,S_\sigma}(\mathbf{x}) = \mathcal{DFT}^{-1}_{(N^3)}\left[\tilde{S}_\sigma(\mathbf{k})\ \tilde{u_i}(\mathbf{k})\right], \tag{2.3}$$

where: $\tilde{S}_\sigma(\mathbf{k}) = \left(1 - \frac{1}{3}\sigma^2\mathbf{k}^2\right)e^{-\frac{1}{2}\sigma^2\mathbf{k}^2}$. It can be shown that with the choice $\sigma = a/\sqrt{5}$, the Gaussian convolution gives the right prefactors for the Faxén correction in the limit $a \to 0$. Our simplified approach for the integration of (1.4) (FC model) allows to track inertial particles in turbulent flows with minimal additional computational costs as compared to Eq. (1.1) (PP model): the fluid acceleration and velocity fields are filtered once for every particle radius size, then the averaged flow at the particle positions are obtained through a tri-linear interpolation. We track particles via Eq. (1.4) in a stationary homogeneous isotropic flow, generated by large-scale volume forcing on a cubic domain. The Navier-Stokes equation is discretized on a regular grid, integrated using a pseudo-spectral algorithm, and advanced in time with a 2$^{\text{nd}}$ order Adams-Bashford integrator.

We have explored in a systematic way the two-dimensional parameter space $[\rho_p/\rho_f, D/\eta]$ in the range $\rho_p/\rho_f \in [0.1, 10]$ and $D/\eta \in [2, 50]$ for a turbulent flow at $Re_\lambda = 180$ (512^3 collocation points). We tracked $\sim 2 \cdot 10^6$ particles for a total of ~ 4 large-eddy turnover time in statistically stationary conditions. Lower resolution DNS at $Re_\lambda = 75$ (128^3) have been used to explore a larger parameter space and to study the differences between the point-particle model (1.1) and the Faxén corrected model (1.4) in the asymptote $D \to L$ (with L the turbulence integral-scale). The validation of the numerics have been performed through careful comparison with an independent code implementing the same algorithm for particles, but with different forcing scheme, temporal integration method (Verlet algorithm), and local interpolation scheme (tri-cubic algorithm).

3. Phenomenology of Point-Particle and Faxén-Corrected models

We compare the statistics of acceleration of particles tracked via the PP and FC equations. In the small particle limit ($D/\eta \to 0$) the two model equations behave the same way and the particle trajectory becomes the one of a fluid tracer. The ensemble-average acceleration variance reaches the value $\langle a^2 \rangle \to \langle a_f^2 \rangle$ with the subscript f labeling

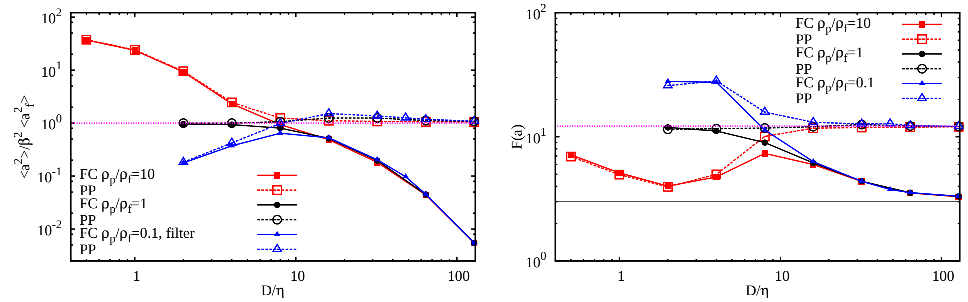

FIGURE 1. (left) The acceleration variance $\langle a^2 \rangle$ normalized by $\beta^2 \langle a_f^2 \rangle$ versus the particle diameter as derived from the Faxén-Corrected model (solid lines/symbols), and from Point-Particle the model system (dashed lines/empty symbols). Density ratios shown are $\rho_p/\rho_f = 0.1, 1, 10$, i.e., heavy ($\square$), neutral ($\circ$) and light ($\triangle$) particles. (right) Same as above for the acceleration flatness $F(a) = \langle a^4 \rangle / \langle a^2 \rangle^2$. Horizontal lines shows the flatness of the fluid acceleration $F(a_f)$ and the flatness value for Gaussian distribution $F(a) = 3$. Data from simulations at $Re_\lambda = 75$.

the fluid tracer acceleration. As the particle diameter is increased we notice important differences between the two models. In the PP model the drag term becomes negligible and one gets $\langle a^2 \rangle \simeq \beta^2 \langle a_f^2 \rangle$, with $\beta = 3\rho_f/(\rho_f + 2\rho_p)$. In the FC model the volume average of the fluid acceleration $D\mathbf{u}/Dt$ reduces progressively the particle acceleration. This is illustrated in Figure 1 (left), where the particle acceleration variance (normalized by $\beta^2 \langle a_f^2 \rangle$) is shown for three cases: neutral buoyant, heavy ($\rho_p/\rho_f = 10$) and light ($\rho_p/\rho_f = 0.1$) particles. We note that the behavior of $\langle a^2 \rangle$ for particles whose diameter is roughly larger than 10η seems to be identical apart from the scaling factor β^2.

Differences are also present in higher order moments: for this we focus on the flatness $F(a) \equiv \langle a^4 \rangle / \langle a^2 \rangle^2$. In the large D limit PP model gives the rather unphysical behavior $F(a) \simeq F(a_f)$, that is to say large particles, irrespectively of their density, show the same level of intermittency as a fluid tracer. On the other hand the Faxén corrected equation gives asymptotically $F(a) \simeq 3$, i.e., the Gaussian flatness value, meaning that acceleration of large particles independently of their mass density value has lost its intermittent character, see Fig. 1 (right). Furthermore, it is noticeable that above a certain critical value of the diameter the flatness of heavy/neutral and light particles reaches the same level: this suggests that also the PDFs may have very similar shapes.

4. Comparison with experiments

We study now how the FC model compares with the experimental observations listed in the introduction – recalling than none is captured by the PP model.

4.1. *Acceleration variance*

In figure 2 the behavior of the one-component acceleration variance, normalized by the Heisenberg-Yaglom scaling, $a_0 = \langle a_i^2 \rangle \epsilon^{-3/2} \nu^{1/2}$, is displayed. Although this way of normalizing the acceleration has a weak Reynolds number dependence (see Voth *et al.* (2002); Bec *et al.* (2006)) we notice a very similar behavior as compared to the experimental measurements at $Re_\lambda = 160$ by Qureshi *et al.* (2007) and with $Re_\lambda = 970$ experiments by Voth *et al.* (2002). In the inset of Figure 2 the same quantity but with a different normalization is shown. The particle acceleration variance there is divided by the second moment of fluid tracer acceleration $\langle a_f^2 \rangle$. The experimental data from Voth *et al.* (2002) can also be rescaled in the same way by dividing a_0 by the value for the smallest considered particle (which has size $D \simeq 1.44\eta$ and essentially behaves as

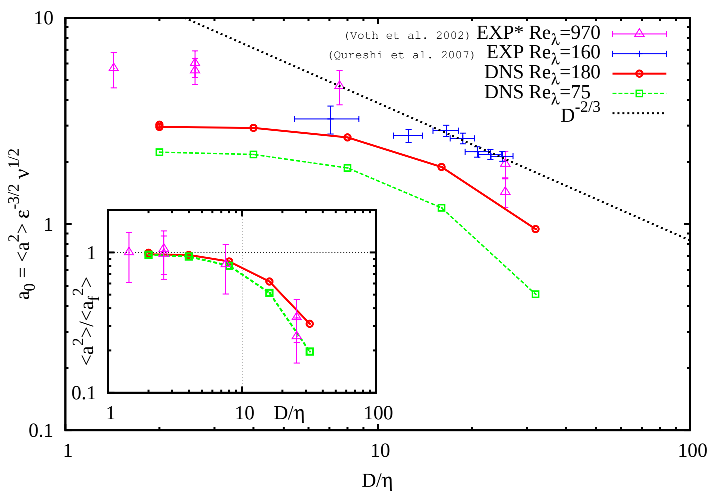

FIGURE 2. One component acceleration variance versus particle size. Acceleration is normalized by the Heisenberg-Yaglom relation, while the particle size is is normalized by the dissipative scale. DNS results have uncertainty of the order of the symbol size. Data EXP are from Qureshi *et al.* (2007), with EXP* measurement from Voth *et al.* (2002) (Figure 32) – particles with density contrast $\rho_p/\rho_f = 1.06$. Inset: $\langle a^2\rangle/\langle a_f^2\rangle$ vs. D/η from the same DNS and EXP* measurements.

a fluid tracer). This alternate way of looking at the data renormalizes the weak Re_λ dependence, providing a good agreement between the DNS and experiments even when comparing results with one order of magnitude difference in Re_λ.

In a DNS one can estimate the relative weight of the terms contributing to the total acceleration: the drag and fluid acceleration terms, respectively: $a^D = (\langle \mathbf{u}\rangle_S - \boldsymbol{v})/\tau_p$ and $a^A = \beta\langle \frac{D\mathbf{u}}{Dt}\rangle_V$. It is important to note that in the case of neutrally buoyant particles, one finds $\langle a\rangle_{rms} \simeq \langle a^A\rangle_{rms}$ with percent accuracy. It indicates that the observed effect - decrease of particle acceleration variance for increasing particle diameter - comes uniquely from volume averaging of fluid acceleration at the particle position. The drag contribution is sub-leading at all D values (from few percent up to 15% of total acceleration variance); it just contributes to compensate the $a^D a^A$ correlations. Stated differently, one can say that the acceleration of a finite-size neutrally buoyant particle is essentially given by $\langle D\mathbf{u}/Dt\rangle_{V_a} = \langle \nabla\cdot\boldsymbol{\tau} + \mathbf{f}_e\rangle_{V_a} \simeq \frac{1}{3a}\langle \boldsymbol{\tau}\cdot\mathbf{n}\rangle_{S_a}$, where $\boldsymbol{\tau}$ is the stress tensor, $\mathbf{n}$ a unit norm vector pointing outward the sphere and $\mathbf{f}_e$ the external large-scale forcing whose contribution $\langle \mathbf{f}_e\rangle_{V_a} \simeq 0$ is negligible at the particle scale. One expects the situation to be different for particles whose density does not match that of the fluid.

Our simulations are consistent with the $a_0 \sim D^{-2/3}$ scaling which has been proposed on the basis of dimensional arguments rooted on Kolmogorov 1941 turbulence phenomenology without special assumptions on particle dynamics (Voth *et al.* (2002); Qureshi *et al.* (2007)); however at $Re_\lambda = 180$ the scale-separation is still too limited to observe a true scaling range.

4.2. *Acceleration probability density function*

The second quantity under study is the acceleration probability density function. Here, to cope with Re_λ effects, one compares only the two most similar data sets: the DNS at $Re_\lambda = 180$ and the experiment at $Re_\lambda = 160$ Qureshi *et al.* (2007). Experiments have revealed a universal behavior for acceleration PDF normalized by $\langle a_i^2\rangle^{1/2}$ in the size-range $D = 12 - 25\eta$. DNS instead shows a systematic difference in the their trend:

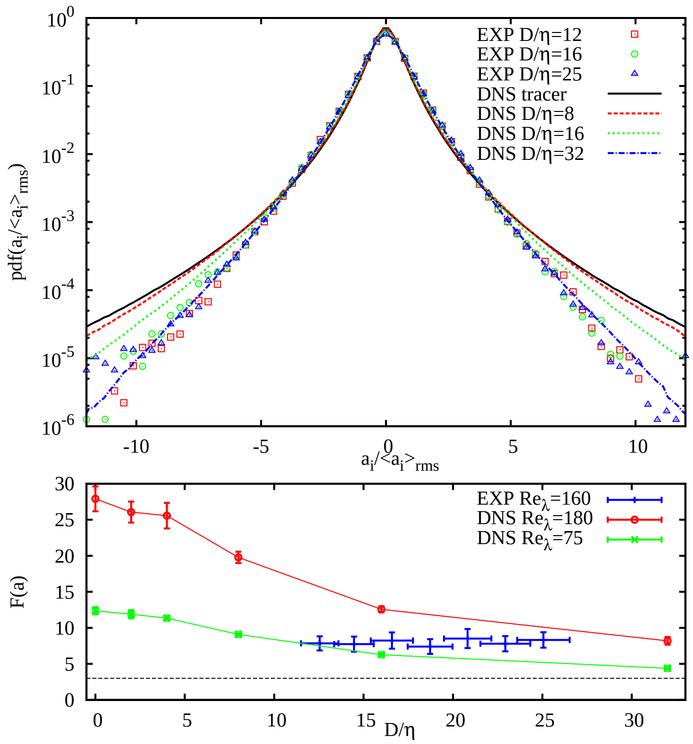

FIGURE 3. (top) Comparison of probability density functions of acceleration normalized by its *rms* value, from EXP Qureshi *et al.* (2007) at $Re_\lambda = 160$ and DNS at $Re_\lambda = 180$. (bottom) One component acceleration flatness $F(a) = \langle a_i^4 \rangle / \langle a_i^2 \rangle^2$ versus the normalized particle diameter, D/η, from the same experiment and DNS at two different Reynolds numbers.

larger particles have less intermittent acceleration statistics, see Figure 3 (top). However, the shape of the PDF in the limit of large particles $D \simeq 30\eta$ shows a good similarity. To better visualize differences, in Figure 3 (bottom), we show the flatness $F(a)$ vs. particle diameter for DNS and experiments. As already observed, the FC model leads to decreasing intermittency for bigger neutral particles, and in the asymptotic limit $(D \to L)$ to Gaussian distribution; also acceleration flatness is an increasing function of Re_λ. Qureshi and coworkers' experiment on the other hand shows a D-independent behavior around $F(a) = 8.5$. A further possible source of differences can be connected to the variations in the large scale properties of turbulent flows: Experimental tracks come from a decaying grid-generated turbulence, simulations instead uses volume large-scale forced flow in a cubic domain without mean flow.

4.3. *Acceleration time-correlation*

Finally, we consider the dynamics of the neutral particles. We study the normalized one-component correlation function, $C_{aa}(\tau) \equiv \langle a_i(t) a_i(t+\tau) \rangle / \langle a_i^2 \rangle$. In Volk *et al.* (2008*a*) it has been noted that PP model can not account for the increasing autocorrelation for larger particles. This is understood from equation (1.1): In the large D limit the drag term is negligible and the acceleration of a neutrally buoyant particle is dominated by the inertial term $D\mathbf{u}/Dt$. Therefore the time-correlation of acceleration, $C_{aa}(\tau)$, is related to the temporal correlation of $D\mathbf{u}/Dt$ along the particle trajectory. Because in the large D limit $\boldsymbol{v} \neq \mathbf{u}$ (Babiano *et al.* (2000)), one expects an acceleration correlation

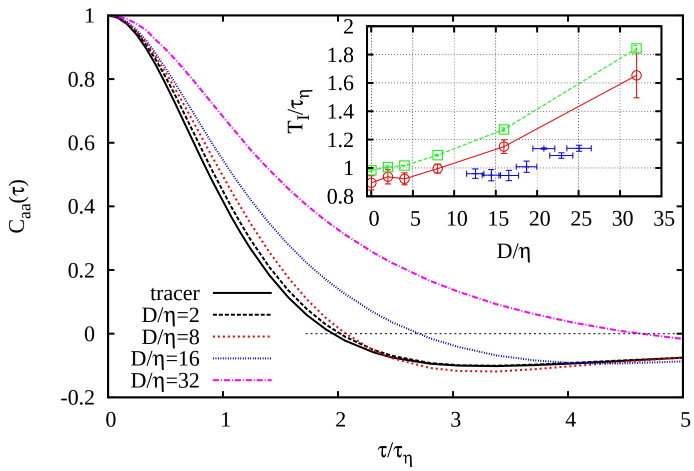

FIGURE 4. Autocorrelation function of acceleration $C_{aa}(\tau)$ for neutral particles ($\rho_p = \rho_f$), with different sizes $D = 2, 8, 16, 32\eta$ and a tracer particle. Inset: integral acceleration time: $T_I = \int_0^{T_0} C_{aa}(\tau)\ d\tau$ with T_0 the zero-crossing time $C_{aa}(T_0) = 0$, versus particle diameter. Symbols: ($\Box$, $\circ$) for DNS at $Re_\lambda = (75, 180)$, data (+) from experiments at $Re_\lambda = 160$.

time which is equal or even shorter than the one of a fluid tracer. This is confirmed by our numerics based on the PP equation (1.1). In the FC model instead, the averaged quantity $\langle D\mathbf{u}/Dt\rangle_{V_a}$ dominates the particle's acceleration and so its time correlation $C_{aa}(\tau)$. In Figure 4 we show that simulations based on Eq. (1.4) display increasing correlation time for bigger particles, as observed in experiment (Volk *et al.* (2008*a*), although at much larger Re_λ values). A detailed comparison of $C_{aa}(\tau)$ curves coming from DNSs with experiments by Qureshi and coworkers is at present not possible, because of limited statistics. Therefore, we examine integral quantities such as an integral acceleration time, T_I. Since by kinematic constraint the time integral of $C_{aa}(\tau)$ for a small tracer is zero, we define T_I as the integral over time of the positive part of $C_{aa}(\tau)$; this choice proves to be stable in the experiments and weakly dependent on the unavoidable (gaussian) smoothing of noisy data sets (see Volk *et al.* (2008*b*)). The result of this analysis is reported in figure 4 (inset). The order of magnitude of T_I/τ_η, which is very near unity, as well its increasing trend with D qualitatively confirms the prediction of the FC model at similar Reynolds number. Using DNS results, it is also interesting to note that this time decreases with increasing Reynolds number.

5. Discussion of results and conclusions

We have investigated the origin of several experimental observations concerning neutrally-buoyant finite-size particle acceleration in turbulent flows and shown the relevance of Faxén corrections. Faxén terms account for inhomogeneities in the fluid flow at the spatial extension of the particle. They act as spatial coarse-graining of the surrounding turbulent flow, in contrast with the drag term which performs a temporal filtering. Numerically, the spatial average is efficiently implemented via Gaussian filtering in spectral space. Comparing with experimental measurements, the main achievements of the Faxén-corrected model are: (i) prediction of the reduction of acceleration fluctuations at increasing the particle size; (ii) prediction of the increasing of acceleration time correlation at increasing the particle size. Both effects originate from the volume average of the fluid acceleration

term, or in other word from the surface average of the stress tensor of the unperturbed flow. While giving the correct trend, the FC model does not solve the puzzling point of invariant PDF with particle size, observed by Qureshi *et al.* (2007).

The Faxén corrected model marks a substantial improvement in the statistical description of realistic turbulent particle suspensions. We emphasize that none of the observed trends in the acceleration of neutrally buoyant particles can be captured by purely local models, as e.g. the point-particle one in eq. (1.1). Faxén corrections are of highest relevance in the case of neutrally buoyant particles, because it is the case for which the slip velocity ($v_s \equiv |\boldsymbol{v} - \langle \mathbf{u} \rangle_S|$) is the smallest (as compared to $\rho_p \neq \rho_f$ particles) and therefore where drag, history , lift have the least impact on the net force. In our case we observe that when increasing the size of particles, the PDFs of slip velocity normalized by the fluid velocity rms value ($v_s/\mathbf{u}_{rms}$) change from a sharp delta-like shape (for tracers) to larger distributions approaching a Gaussian (for large particles). A size-dependent slip velocity for neutrally buoyant tracers in chaotic flows has been reported recently in Ouellette *et al.* (2008): Faxén corrections to the added mass should be significant in that case too. We also observe that the particle-Reynolds number Re_p measured in our simulations attains values in the order of the hundreds, hence a more accurate description of the drag coefficient (see for instance Clift *et al.* (1978)) may be important particularly for a faithful reproduction of the far tails of the acceleration PDF.

Acknowledgments: The authors acknowledge the Grenoble team (N. M. Qureshi, C. Baudet, A. Cartellier and Y. Gagne) for generously sharing their experimental data measurements, and J.Bec for useful discussions. Numerical simulations were performed at SARA (The Netherlands), CINECA (Italy) and PSMN, ENS-Lyon (France). Numerical raw data on FC particles are freely available on iCFDdatabase (http://cfd.cineca.it) kindly hosted by CINECA (Italy).

REFERENCES

Arneodo, A., Benzi, R., Berg, J., Biferale, L., Bodenschatz, E., Busse, A., Calzavarini, E., Castaing, B., Cencini, M., Chevillard, L., Fisher, R. T., Grauer, R., Homann, H., Lamb, D., Lanotte, A. S., Leveque, E., Luthi, B., Mann, J., Mordant, N., Muller, W. C., Ott, S., Ouellette, N. T., Pinton, J. F., Pope, S. B., Roux, S. G., Toschi, F., Xu, H. & Yeung, P. K. 2008 Universal intermittent properties of particle trajectories in highly turbulent flows. *Phys. Rev. Lett.* **100** (25), 254504–5.

Auton, T., Hunt, J. & Prud'homme, M. 1988 The force exerted on a body in inviscid unsteady non-uniform rotational flow. *J. Fluid Mech.* **197**, 241–257.

Ayyalasomayajula, S., Gylfason, A., Collins, L. R., Bodenschatz, E. & Warhaft, Z. 2006 Lagrangian measurements of inertial particle accelerations in grid generated wind tunnel turbulence. *Phys. Rev. Lett.* **97**, 144507.

Babiano, A., Cartwright, J. H. E., Piro, O. & Provenzale, A. 2000 Dynamics of a small neutrally buoyant sphere in a fluid and targeting in hamiltonian systems. *Phys. Rev. Lett.* **84** (25), 5764–5767.

Balkovsky, E., Falkovich, G. & Fouxon, A. 2001 Intermittent distribution of inertial particles in turbulent flows. *Phys. Rev. Lett.* **86** (13), 2790–2793.

Bec, J. 2005 Multifractal concentrations of inertial particles in smooth random flows. *J. Fluid Mech.* **528**, 255–277.

Bec, J., Biferale, L., Boffetta, G., Celani, A., Cencini, M., Lanotte, A., Musacchio, S. & Toschi, F. 2006 Acceleration statistics of heavy particles in turbulence. *J. Fluid Mech.* **550**, 349–358.

Berg, J. 2006 Lagrangian one-particle velocity statistics in a turbulent flow. *Phys. Rev. E* **74**, 016304.

Biferale, L., Bodenschatz, E., Cencini, M., Lanotte, A. S., Ouellette, N. T., Toschi,

F. & Xu, H. 2008 Lagrangian structure functions in turbulence: A quantitative comparison between experiment and direct numerical simulation. *Phys. Fluids* **20** (6), 065103.

Calzavarini, E., Cencini, M., Lohse, D. & Toschi, F. 2008*a* Quantifying turbulence-induced segregation of inertial particles. *Phys. Rev. Lett.* **101**, 084504.

Calzavarini, E., Kerscher, M., Lohse, D. & Toschi, F. 2008*b* Dimensionality and morphology of particle and bubble clusters in turbulent flow. *J. Fluid Mech.* **607**, 13–24.

Clift, R., Grace, J. R. & E., W. M. 1978 *Bubbles, drops and particles*. New York: Academic Press.

Faxén, H. 1922 *Ann. Phys. (Leipzig)* **4** (LXVIII), 89.

Gatignol, R. 1983 The faxén formulae for a rigid particle in an unsteady non-uniform stokes flow. *J. Mecanique Theorique et Appliquée* **1** (2), 143–160.

La Porta, A., Voth, G. A., Crawford, A. M., Alexander, J. & Bodenschatz, E. 2001 Fluid particle accelerations in fully developed turbulence. *Nature* **409**, 1017.

Magnaudet, J. & Legendre, D. 1998 Some aspects of the lift force on a spherical bubble. *Appl. Sci. Res.* **58**, 441.

Maxey, M. R. & Riley, J. J. 1983 Equation of motion for a small rigid sphere in a nonuniform flow. *Phys. Fluids* **26** (4), 883–889.

Michaelides, E. E. 1997 Review - the transient equation of motion for particles, bubbles, and droplets. *J. Fluid Eng.* **119**, 233–247.

Mordant, N., Lévêque, E. & Pinton, J. F. 2004 Experimental and numerical study of the lagrangian dynamics of high reynolds turbulence. *New J. Physics* **6**, 116.

Mordant, N., Metz, P., Michel, O. & Pinton, J.-F. 2001 Measurement of lagrangian velocity in fully developed turbulence. *Phys. Rev. Lett.* **87** (21), 214501.

Ouellette, N. T., O'Malley, P. J. J. & Gollub, J. P. 2008 Transport of finite-sized particles in chaotic flow. *Phys. Rev. Lett.* **101**, 174504.

Qureshi, N. M., Bourgoin, M., Baudet, C., Cartellier, A. & Gagne, Y. 2007 Turbulent transport of material particles: An experimental study of finite size effects. *Phys. Rev. Lett.* **99** (18), 184502.

Salazar, J., de Jong, J., Cao, L., Woodward, S., Meng, H. & Collins, L. 2008 Experimental and numerical investigation of inertial particle clustering in isotropic turbulence. *J. Fluid Mech.* **600**, 245 – 256.

Squires, K. D. & Eaton, J. K. 1991 Preferential concentration of particles by turbulence. *Phys. Fluids A* **3** (5), 1169–1179.

Toschi, F. & Bodenschatz, E. 2009 Lagrangian properties of particles in turbulence. *Ann. Rev. Fluid Mech.* **41**, 375–404.

Volk, R., Calzavarini, E., Verhille, G., Lohse, D., Mordant, N., Pinton, J. F. & Toschi, F. 2008*a* Acceleration of heavy and light particles in turbulence: comparison between experiments and direct numerical simulations. *Physica D* **237** (14-17), 2084–2089.

Volk, R., Mordant, N., Verhille, G. & Pinton, J. F. 2008*b* Laser doppler measurement of inertial particle and bubble accelerations in turbulence. *Europhys. Lett.* **81** (3).

Voth, G. A., La Porta, A., Crawford, A. M., Alexander, J. & Bodenschatz, E. 2002 Measurement of particle accelerations in fully developed turbulence. *J. Fluid Mech.* **469**, 121–160.

Xu, H., Bourgoin, M., Ouellette, N. T. & Bodenschatz, E. 2006 High order lagrangian velocity statistics in turbulence. *Phys. Rev. Lett.* **96** (2), 024503.